

# Diagnostic Role of Diffusion Tensor Imaging in Brain Cancers

Hossnia A. Mohamed, Manal F. Khaled , Aya E. Mohamed \*

Department of Radiodiagnosis, Faculty of Medicine for Girls, Al-Azhar University, Cairo, Egypt

## Abstract

**Background:** Magnetic resonance (MR) imaging, in particular, has emerged as the imaging modality most commonly utilized to assess intracranial cancers.

**Aim:** To assess the role of the recent magnetic resonance imaging tools, such as Diffusion Tensor Imaging and Fiber Tractography, in brain neoplasm diagnosis.

**Cases and methods:** This investigation involved 40 cases diagnosed with brain cancers dependent on conventional magnetic resonance imaging referred from neurosurgery department to magnetic resonance imaging unite in radio-diagnosis department at Al Zahraa University Hospitals in the period between March 2021 to March 2023.

**Results:** There was statistically significance as regard diffusion tensor imaging metrics in differentiation between different pathological subtypes were greater mean value of FA in low grade glioma was  $0.48 \pm 0.07$ , followed by metastatic deposits was  $0.41 \pm 0.03$ , then high grade glioma was  $0.24 \pm 0.07$ , with  $p$ -value ( $p < 0.001$ ), greater mean value of ADC ( $\times 10^3$  "mm<sup>2</sup>/sec") in high grade glioma was  $2.00 \pm 0.29$ , followed by metastatic deposits was  $1.58 \pm 0.44$ , then low grade glioma was  $1.13 \pm 0.29$ , with  $p$ -value ( $p < 0.001$ ).

**Conclusion:** We concluded that the evaluation of the impact of cerebral neoplasms on white matter pathways is significantly more accurate with the assistance of DTI than with conventional magnetic resonance imaging. A cancer may cause one or more of four distinct patterns change of white matter tract. DTI has the potential to be used in the characterization of cancers, and more importantly, in the operative procedures planning.

**Keywords:** Fractional anisotropy (FA); Diffusion Tensor Imaging (DTI); Mean diffusivity (MD)

## 1. Introduction

In particular, magnetic resonance imaging became the imaging modality that is most commonly utilized to assess intracranial cancer; it plays a multifaceted and ever-expanding role. Generally, the function of magnetic resonance imaging in intraaxial cancers evaluation may be broadly classified into three categories: classification and diagnosis of cancer, management planning, and post-treatment surveillance.<sup>1</sup>

Imaging is essential for the management of intracranial cancers. In cases with brain cancers, the preoperative planning and evaluation of nearby white matter (WM) tracts is

a critical step in enabling the complete resection of the cancer, while simultaneously preventing the recurrence of the cancer and the loss of vital brain functions, including sensory, motor, language, auditory, and visual fields.<sup>2</sup>

Currently, the only available instrument that demonstrates disruption of white matter tracts by fractional anisotropy alterations and the reconstruction of fibers in cases of malignant brain cancers is diffusion-tensor imaging with tractography. Therefore, it is essential to precisely identify white matter tracts to facilitate preoperative planning and determine whether or not to perform the operation.<sup>3</sup>

Accepted 06 February 2025.  
Available online 28 February 2025

\* Corresponding author at: Radiodiagnosis, Faculty of Medicine for Girls, Al-Azhar University, Cairo, Egypt.  
E-mail address: [Rabeaaya639@gmail.com](mailto:Rabeaaya639@gmail.com) (A. E. Mohamed).

<https://doi.org/10.21608/aimj.2025.446435>

2682-339X/© 2024 The author. Published by Al-Azhar University, Faculty of Medicine. This is an open access article under the CC BY-SA 4.0 license (<https://creativecommons.org/licenses/by-sa/4.0/>).

The effectiveness of diffusion methods is derived from the tissue structures' molecular probing by H<sub>2</sub>O molecules at a microscopic scale that exceeds the usual resolution of magnetic resonance imaging. In terms of mean diffusivity and fractional anisotropy, it measures the water diffusivity average and directional variation for a particular voxel, corresponding to providing information about tissue architecture and microstructure.<sup>4</sup>

We aimed in this study to assess the role of the recent magnetic resonance imaging tools, such as Diffusion Tensor Imaging and Fiber Tractography, in brain neoplasm diagnosis.

## 2. Patients and methods

This investigation involved 40 cases diagnosed with brain cancers depending on conventional magnetic resonance imaging referred from neurosurgery department to magnetic resonance imaging unite in radio-diagnosis department at Al Zahraa University Hospitals in the period between March 2021 to March 2023.

**Inclusion criteria:** Cases of the population undergo magnetic resonance imaging scanning with clinically suspected brain cancers or having previous investigation, such as computed tomography, and Cases older than 10 years.

**Exclusion criteria:** Cases who are contraindicated to perform magnetic resonance imaging: Cases with intraocular metallic foreign body, Cases with heart pace makers, Cases with magnetic resonance non compatible arterial brain aneurysms intracranial clips, Cases having history of claustrophobia and Cases clinically unstable.

### Methods

Patients were grouped according to the pathological findings into the following: There were twelve cases of intra-axial low-grade gliomas, involving WHO grade I and II, six cases of grade I, and six cases of grade II. There were twenty-three cases of intra-axial high-grade gliomas, involving WHO grade III and IV, ten cases of grade III, and thirteen cases of grade IV. There were also five cases of intra-axial metastatic cancers of known 1ry origin (bronchogenic, colonic & breast cancers).

Each patient involved in the investigation was subjected to:

Neurological clinical examination, complete history taking, general examination, and magnetic resonance examination involving

Before and after contrast conventional magnetic resonance examination involving T1WI, T2WI, & FLAIR in axial, coronal and sagittal planes and DTI with fiber tracking (Tractography).

### MRI Technique

The method has been carried out with a 1.5 Tesla scanner (Philips, Ingenia) and a 20-channel,

head-neck coil.

Sequences acquired were sagittal, axial, & coronal T1W, T2W, FLAIR, and following intravenous contrast T1 images. Gadoterate meglumine 0.5 milliliters per kilogram (0.1 millimoles per kilogram body weight with a maximum dose of ten milliliters has been administered intravenously as a bolus injection at a flow rate of around two milliliters per second utilizing a twenty to twenty-two G venous cannula. The diffusion tensor has been composed of a single-shot, spin-echo echoplanar sequence in sixteen encoding directions and a diffusion weighting factor of eight hundred seconds per millimeter square. The sequence parameters are as follows: T1WI: TR = 600 millisecond, TE = 25 millisecond, matrix 80 x 80, FOV 250 x 170, slice thickness five millimeters, T2WI: TR = 6000 millisecond, TE 90 = millisecond, matrix 80 x 80, FOV 250 x 170, thickness of slice five millimeters, FLAIR: TR = 10,000 millisecond, TE = 115 millisecond, TI = 2700 millisecond, matrix 80 x 80, FOV 250 x 170, thickness of slice five millimeters, DTI: The diffusion tensor imaging data have been acquired utilizing a single-shot echo planar imaging sequence (TR/TE 3200/90 millisecond) with parallel imaging (SENSitivity Encoding [SENSE] reduction factor P 2). The p-value was set to zero, and the diffusion gradients have been applied along twenty axes at a rate of a thousand seconds per millimeter square. Voxel dimensions (2.43× 2.54 × 2.5 cubic millimeters) have been achieved by utilizing a 92 × 88 data matrix and a field of view (FOV) of 224 × 224 square millimeters. The total scan period was approximately between seven and eight minutes, and forty-eight slices were gathered with a thickness of 2.5 millimeters and no gap.

### Post processing

The DICOM images have been transmitted to the workstation (Extended Magnetic Resonance Workspace 12.1.5.1, Philips Medical Systems). The eddy current artifacts have been eliminated by automating the registration of the DTI data. The ellipsoid ROI technique has been utilized to measure metrics in the solid region of the various pathological groups (metastases and gliomas), involving the mean diffusivity and fractional anisotropy. A specific color is designated to tracts that run in the three orthogonal planes: red for right-to-left tracts, green for anteroposterior tracts, and blue for craniocaudal tracts. Anatomy and direction of the tracts are visible in the directionally encoded Fractional anisotropy maps. Tracts have been created in three dimensions. An ROI (or seed) has been drawn (placed) along the tract course in a color-encoded Fractional anisotropy map in single or consecutive sections to create 3D fiber tracts. Subsequently, the software generates a 3D model of the

assigned tract. The cancer-related tracts have been assessed in accordance with their pattern of involvement. The tractography program's algorithm has been designed for tracts that were greater than ten millimeters, angles that were less than twenty-seven degrees, and a fractional anisotropy threshold that was greater than 0.15.

Method of tracking the different anatomical tracts

Corticospinal tract: 3 ROIs have been placed on transverse color-coded diffusion tensor images: one in the anterior pons, the second in the posterior internal capsule, and the third in the motor cortex. Superior longitudinal fasciculus: 2 ROIs have been placed in cerebral deep white matter using a coronal directional color-coded map, one in the reconstructed corticospinal tract and the other in the rostral corpus callosum splenium. Inferior longitudinal fasciculus: 2 ROIs have been identified in the parieto-occipital sulcus and mid-temporal lobe, located in the inferior axis and posterior tip of the putamen, respectively.

#### Statistical analysis

The statistical package for social sciences, version 23.0 (SPSS Inc., Chicago, Illinois, United States of America), has been utilized to analyze information that has been recorded. Mean± standard deviation and ranges have been utilized to present quantitative data. Additionally, percentages and numbers have been utilized to present qualitative variables. The Shapiro-Wilk Test and the Kolmogorov-Smirnov Test have been utilized to explore the normality of the data. The subsequent tests have been done: The margin of error accepted was set to five percent, and the confidence interval was set to ninety-five percent for a one-way analysis of variance (ANOVA), Chi-square test, and Fisher's exact test. Therefore, the p-value has been deemed significant if the probability (P-value) was less than 0.05, highly significant if the P-value was less than 0.001, and insignificant if the P-value was greater than 0.05.

### 3. Results

Age varied from 26 to 68 years with mean± SD of 51.08±10.74. There were 6 cases (15.0%) were <40 years, 12 cases (30.0%) were 40-50 years, 14 cases (35.0%) were >50-60 years and 8 cases (20.0%) were >60 years between age group; Regarding gender distribution, there was female predominance with 24 females with percentage 60% and 16 males with percentage 40%. (Table 1)

Table 1. Baseline characteristics distribution between study group.

DEMOGRAPHIC DATA	NO.	%
AGE GROUP		
<40 YEARS	6	15.0%
40-50 YEARS	12	30.0%

>50-60 YEARS	14	35.0%
>60 YEARS	8	20.0%
GENDER		
FEMALE	24	60.0%
MALE	16	40.0%

13 cases (32.5%) were diagnosed as glioblastoma multiforme, 8 cases (20.0%) were anaplastic astrocytoma, 6 cases (15.0%) were diffuse astrocytoma, 5 cases (12.5%) were metastatic deposits, 4 cases (10.0%) were low grade astrocytoma, 2 cases (5.0%) were intermediate glioma and 2 cases (5.0%) were low grade glioma between pathological diagnosis of lesions. (Table 2)

Table 2. Pathological diagnosis of lesions distribution between study group.

PATHOLOGICAL DIAGNOSIS OF LESIONS	NO.	%
GLIOBLASTOMA MULTIFORME	13	32.5%
ANAPLASTIC ASTROCYTOMA	8	20.0%
DIFFUSE ASTROCYTOMA	6	15.0%
METASTATIC DEPOSITS	5	12.5%
LOW GRADE ASTROCYTOMA	4	10.0%
INTERMEDIATE GLIOMA	2	5.0%
LOW GRADE GLIOMA	2	5.0%
TOTAL	40	100.0%

FA range was 0.14-0.562 with mean 0.33±0.13 and ranged of ADC ( $\times 10^3$  "mm<sup>2</sup>/sec") 0.7-2.5 with mean 1.69±0.49. (Table 3)

Table 3. FA and ADC ( $\times 10^3$  "mm<sup>2</sup>/sec") distribution between study group.

TOTAL (NUMBER=40)	
FA	
RANGE	0.14-0.562
MEAN±SD	0.33±0.13
ADC ( $\times 10^3$ "MM <sup>2</sup> /SEC")	
RANGE	0.7-2.5
MEAN±SD	1.69±0.49

There was highly statistically significant greater FA mean value in low grade glioma was 0.48±0.07, followed by metastatic deposits was 0.41±0.03, then high grade glioma was 0.24±0.07, with p-value (p-value less than 0.001). (Table 4)

Table 4. Comparison among various cancer grades & FA.

FA	LOW GRADE GLIOMA (NUMBER=12)	HIGH GRADE GLIOMA (NUMBER=23)	METASTATIC DEPOSITS (NUMBER=5)	F-TEST	P-VALUE
MEAN±SD	0.48±0.07A	0.24±0.07C	0.41±0.03B	52.939	<0.001**
RANGE	0.36-0.56	0.14-0.41	0.38-0.43		

utilizing: One-way Analysis of Variance test has been carried out for Mean±SD & Multiple comparison among groups utilizing Post Hoc test: Tukey's test Different capital letters show significant distinction at (p-value less than 0.05) between means in same row \*\*p-value less than 0.001 is highly significant



There was highly statistically significant greater ADC mean value ( $\times 10^3$  "mm<sup>2</sup>/sec") in high grade glioma was  $2.00 \pm 0.29$ , followed by metastatic deposits was  $1.58 \pm 0.44$ , then low grade glioma was  $1.13 \pm 0.29$ , with p-value (p-value less than 0.001). (Table 5)

Table 5. Comparison among various cancer grades & ADC ( $\times 10^3$  "mm<sup>2</sup>/sec").

ADC ( $\times 10^3$ "MM <sup>2</sup> /SEC")	LOW GRADE GLIOMA (NUMBER=12)	HIGH GRADE GLIOMA (NUMBER=23)	METASTATIC DEPOSITS (NUMBER=5)	F-TEST	P-VALUE
MEAN $\pm$ SD	1.13 $\pm$ 0.29C	2.00 $\pm$ 0.29A	1.58 $\pm$ 0.44B	32.133	<0.001**
RANGE	0.7-1.5	1.6-2.5	1.1-1.9		

### CASE PRESENTATION

Case One: Male case aged 48 years presented with headache right side hemiparesis and signs of increase intracranial tension.

#### Conventional MRI

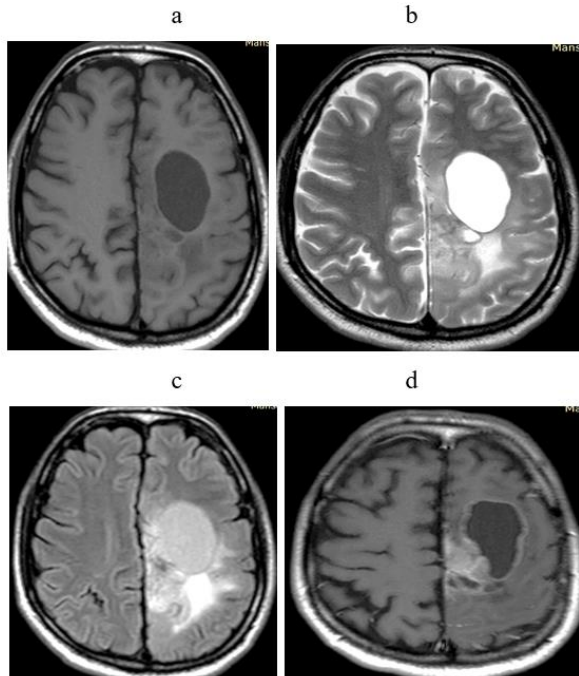


Figure 1. a) Axial T1 image showing low signal of the cancer. b) Axial T2 image showing left fronto-parietal SOL with surrounding edema and large cystic part with related sulci effacement, c) Axial FLAIR image demonstrating the high signal of the cancer with mild peri-cancerous edema d) axial T1 post contrast images demonstrating areas of nodular and marginal cancer enhancement.

#### Diffusion tensor imaging maps

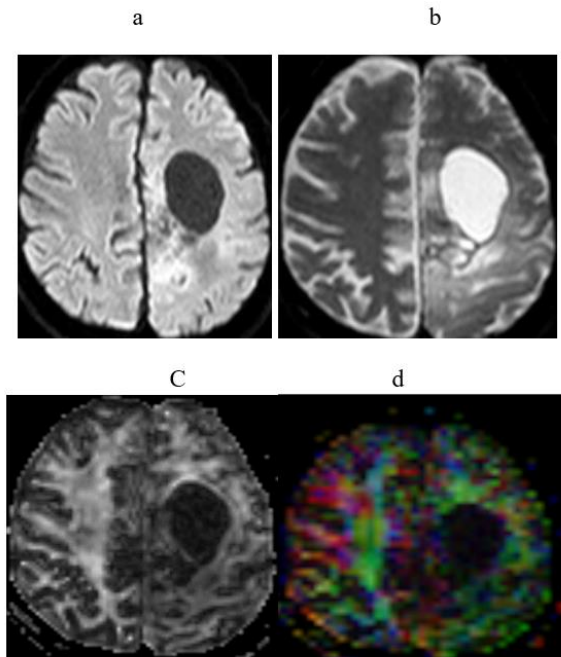


Figure 2. a) Axial DWI demonstrating facilitated diffusion. b) Axial ADC maps demonstrating high signal of lesion. c) Axial FA map demonstrating low signal of lesion. d) axial FA color demonstrating color disorganization.

#### Tractography

Projection fibers: Disruption of the upper fibers of the left corticospinal tracts.

Commissural fibers: Disrupted the left side of the corpus callosum fibers.

Association fibers: Partial disruption of the left cerebral fasciculi.

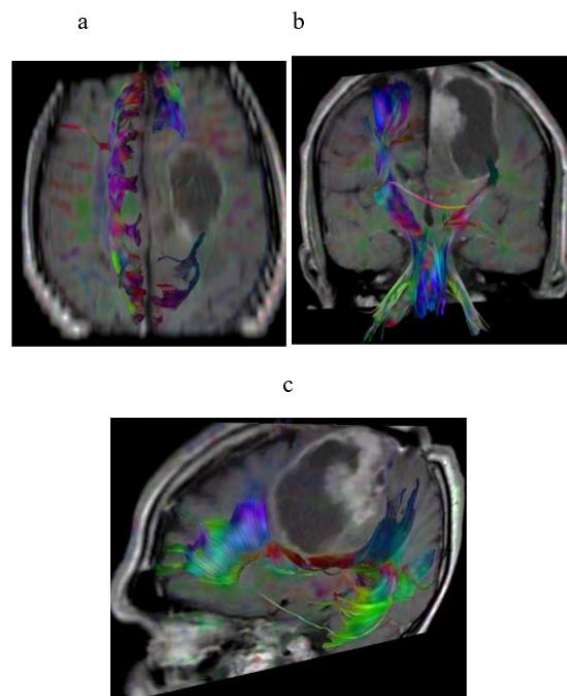


Figure 1. a) MIP axial image of the corticospinal tracts in with interruption of the left tract. b) MIP

coronal image demonstrating disrupted left CST. c) 3D with sagittal image and lateral view demonstrating left corpus callosum fibers and fasciculi disruption.

#### 4. Discussion

Regarding the demographic and clinical data in our study, age varied from 26 to 68 years with a mean $\pm$ SD of 51.08 $\pm$ 10.74. There were 6 cases (15.0%) were <40 years, 12 cases (30.0%) were 40-50 years, 14 cases (35.0%) were >50-60 years and 8 cases (20.0%) were >60 years between age group; Regarding gender distribution, there was female predominance with 24 females with percentage 60% and 16 males with percentage 40%. Between the clinical presentation there were 33 cases (82.5%) presented by motor weakness, 32 cases (80.0%) by headache, 30 cases (75.0%) by convulsion, 19 cases (47.5%) by visual symptoms, 12 cases (30.0%) by dysarthria, 12 cases (30.0%) by hemiparesis, 10 cases (25.0%) by behavioral change and 5 cases (12.5%) by ataxia. According to the diagnosis of the lesions, there were 12 cases (30.0%) who had low-grade glioma; 23 cases (57.5%) had high-grade glioma, and 5 cases (12.5%) were metastatic deposits. Regarding WHO grading of the lesions, 6 cases (17.1%) were Grade I, 6 cases (17.1%) were Grade II, 10 cases (28.6%) were Grade III, and 13 cases (37.1%) were Grade IV.

In a similar study by Ibrahim et al.,<sup>5</sup> The age varied from one to seventy-four years old, and the mean age was 32.8  $\pm$  18. Most of the cases examined were men (68.8%) and were over the age of forty. Hemiparesis was the most common neurological clinical manifestation. The cancers in question included three low-grade gliomas, ten grade II-III gliomas, two grade III gliomas, five glioblastoma multiforme, three gliomatosis cerebri, three metastases, one lymphoma, three brain stem gliomas, and two meningiomas.

Our analysis of the affected white matter tracts showed that the most important studied WM tract is the corticospinal tract (CST) due to its crucial importance for motor function and sparing during surgery. It was involved in 35 cases (87.5%). Other WM tracts affected in this study included the corpus callosum in 26 cases (65%), the superior longitudinal (arcuate) fasciculus in 25 cases (62.5%), inferior longitudinal fasciculus in 18 cases (45%), superior fronto-occipital fasciculus in 15 case (37.5%)., inferior fronto-occipital fasciculus in 10 cases (25%) and medial lemniscus in 3 cases (7.5%). It should be noted that many cases showed involvement of more than one tract.

We characterized the pattern of WM tract involvement and found that

deviation/displacement of WM tracts was by far the most common pattern of WM tract involvement seen in a total of 28 (70%) cases: 16 low-grade, 9 high-grade cancers and 3 cases of metastatic deposits. While edematous WM tracts were seen in 16 (40%) cases: 5 low-grade, 9 high-grade cancers and 2 cases of metastatic deposits. WM tract infiltration was seen in 12 (30%) cases: 2 low-grade, 8 high-grade cancers and 2 cases of metastatic deposits. Finally, nine cases (22.5%) showed WM tract interruption: all of high-grade cancers.

This pattern's classification of tract involvement was comparable to investigations conducted by Ibrahim et al.<sup>5</sup> & Witwer et al.<sup>6</sup>

Nevertheless, this was slightly different from the classification carried out by Yu et al.<sup>7</sup> who divided association between cancer and tracts into 3 types; type I: simple displacement, type II: displacement with disruption, and type III: simple disruption.

Numerous reports exist in the literature on the application of Diffusion Tensor Imaging and its guidance for craniotomy with functional magnetic resonance imaging and during surgery navigation. Earlier investigations stated that preoperative diffusion tensor imaging may impact the surgical strategy choice, and with a combination of during surgery diffusion tensor imaging and navigation, surgeons can better resect cancers and protect neurological function Sun et al.,<sup>8</sup>; Muthusami et al.,<sup>9</sup>

In addition, D'Andrea et al.<sup>10</sup> utilized preoperative Diffusion Tensor Imaging for cases with glioma near the right lateral temporal lobe to demonstrate cancer and optic fascicle spatial shape.

Regarding the involvement of four patterns of white matter fiber tracts in our investigation, DTI showed great ability to differentiate between low grade glioma, high grade glioma and metastatic deposits.

Our results show a statistical distinction between these groups, with displacement occurrence between benign group and edema occurrence, infiltration and disruption between malignant group.

These results are partially in agreement with the results of Ibrahim et al.,<sup>5</sup> There was a statistical difference in the occurrence of displacement between the benign group and disruption between the malignant group, with a P-value less than 0.05. This, in contrast to edema impact and infiltration, where there was an insignificant distinction between both groups, with P-value more than 0.05 Our quantitative DTI metrics assessment showed that the range of Fractional Anisotropy (FA) 0.14-0.562 with mean 0.33 $\pm$ 0.13 and range of ADC ( $\times 10^{-3}$  "mm<sup>2</sup>/sec") 0.7-2.5 with mean 1.69 $\pm$ 0.49.

Our results also revealed statistically significantly greater mean value of AF in low-grade glioma was  $0.48 \pm 0.07$ , followed by metastatic deposits was  $0.41 \pm 0.03$ , then high-grade glioma was  $0.24 \pm 0.07$ , with p-value ( $p < 0.001$ ).

According to Chen et al.,<sup>11</sup> the Fractional anisotropy value is an indicator of white matter integrity and decreased Fractional anisotropy was putative destruction of white matter tract. Nevertheless, studying the association between the Fractional anisotropy values of LGG and HGG is still controversial.

In addition, our results show a highly statistically significant greater mean value of ADC ( $\times 10^3$  "mm<sup>2</sup>/sec") in high-grade glioma was  $2.00 \pm 0.29$ , followed by metastatic deposits, which was  $1.58 \pm 0.44$ , then low-grade glioma, which was  $1.13 \pm 0.29$ , with p-value ( $p < 0.001$ ).

Sinha et al.<sup>12</sup> discovered a significant distinction in ADC values between apparently normal white matter, edematous brain, and improving cancer margins. Diffusion anisotropy information did not provide any benefit in tissue differentiation.

Increased ADC and decreased Fractional anisotropy have been reported by Berman et al.<sup>13</sup> to reflect a combination of vasogenic edema and cancer infiltration. Report of the CST, including areas of edema or cancer, showing low Fractional anisotropy might represent fiber disruption on a Fractional anisotropy map. Their outcomes also supported an association between reduced Fractional anisotropy and increased ADC with CST involvement.

#### 4. Conclusion

We came to a conclusion that the cerebral neoplasms impact on white matter pathways is more effectively assessed using diffusion tensor imaging than conventional magnetic resonance imaging. A cancer may cause one or more of four distinct patterns change of white matter tract. DTI has the potential to play a role in classification of cancer, and more significantly, in the surgical procedures planning.

#### Disclosure

The authors have no financial interest to declare in relation to the content of this article.

#### Authorship

All authors have a substantial contribution to the article

#### Funding

No Funds : Yes

#### Conflicts of interest

There are no conflicts of interest.

#### References

1. Zhang H, Feng Y, Cheng L, Liu J, Li H, Jiang H. Application of diffusion tensor tractography in the surgical treatment of brain cancers located in functional areas. *Oncol Lett*. 2020 Jan;19(1):615-622.
2. Wang LL, Leach JL, Breneman JC, McPherson CM, Gaskill-Shiple MF. Critical role of imaging in the neurosurgical and radiotherapeutic management of brain cancers. *Radiographics*. 2014 May-Jun;34(3):702-21.
3. Farahat AH, Lgohary ME, Hafez H. The Role of the Diffusion Tensor Imaging and the MR Tractography in the Evaluation of the Ischemic Cerebral Strokes. *Int. J. Radiol. Imaging Technol*. 2018;4:1-7.
4. Mahmoud BE, Mohammad ME, Serour DK. What can DTI add in acute ischemic stroke cases?. *Egyptian Journal of Radiology and Nuclear Medicine*. 2019 Dec;50:1-8.
5. Ibrahim AS, Gomaa M, Sakr H, Abd Elzaher Y. Role of diffusion tensor imaging in characterization and preoperative planning of brain neoplasms. *The Egyptian Journal of Radiology and Nuclear Medicine*. 2013 Jun 1;44(2):297-307.
6. Witwer BP, Moftakhar R, Hasan KM, Deshmukh P, Haughton V, Field A, Arfanakis K, Noyes J, Moritz CH, Meyerand ME, Rowley HA, Alexander AL, Badie B. Diffusion-tensor imaging of white matter tracts in cases with cerebral neoplasm. *J Neurosurg*. 2002 Sep;97(3):568-575.
7. Yu CS, Li KC, Xuan Y, Ji XM, Qin W. Diffusion tensor tractography in cases with cerebral cancers: a helpful technique for neurosurgical planning and postoperative assessment. *Eur J Radiol*. 2005 Nov;56(2):197-204.
8. Sun GC, Chen XL, Zhao Y, Wang F, Hou BK, Wang YB, et al. Intraoperative high-field magnetic resonance imaging combined with fiber tract neuronavigation-guided resection of cerebral lesions involving optic radiation. *Neurosurgery*. 2011 Nov;69(5):1070-84; discussion 1084.
9. Muthusami P, James J, Thomas B, Kapilamoorthy TR, Kesavadas C. Diffusion tensor imaging and tractography of the human language pathways: moving into the clinical realm. *J Magn Reson Imaging*. 2014 Nov;40(5):1041-1053.
10. D'Andrea G, Familiari P, Di Lauro A, Angelini A, Sessa G. Safe Resection of Gliomas of the Dominant Angular Gyrus Awaiting of Preoperative FMRI and Intraoperative DTI: Preliminary Series and Surgical Technique. *World Neurosurg*. 2016 Mar;87:627-639.
11. Chen L, Zou X, Wang Y, Mao Y, Zhou L. Central nervous system cancers: a single center pathology review of 34,140 cases over 60 years. *BMC Clin Pathol*. 2013 May 2;13(1):14.
12. Sinha S, Bastin ME, Whittle IR, Wardlaw JM. Diffusion tensor MR imaging of high-grade cerebral gliomas. *AJNR Am J Neuroradiol*. 2002 Apr;23(4):520-527.
13. Berman JI, Berger MS, Mukherjee P, Henry RG. Diffusion-tensor imaging-guided tracking of fibers of the pyramidal tract combined with intraoperative cortical stimulation mapping in cases with gliomas. *J Neurosurg*. 2004 Jul;101(1):66-72.